ELSEVIER

Contents lists available at ScienceDirect

# Chemical Engineering Journal

journal homepage: www.elsevier.com/locate/cej

Chemical Engineering Journal

# A comparative study of CO<sub>2</sub> diffusion from adsorption kinetic measurements on microporous materials at low pressures and temperatures



S.I. Garcés-Polo<sup>a</sup>, J. Villarroel-Rocha<sup>b</sup>, K. Sapag<sup>b</sup>, S.A. Korili<sup>a</sup>, A. Gil<sup>a,\*</sup>

<sup>a</sup> Departamento de Química Aplicada, Edificio de los Acebos, Universidad Pública de Navarra, Campus de Arrosadía, 31006 Pamplona, Spain

#### HIGHLIGHTS

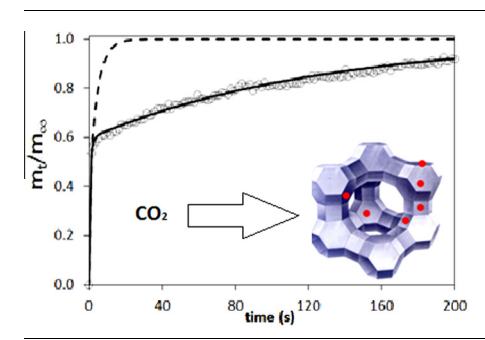
- $\bullet$  Adsorption kinetics of  $CO_2$  on several microporous materials at 273–293 K and up to 100 kPa.
- Isothermal and non-isothermal models used to calculate diffusion coefficients.
- Darken equation and a structural model used to study the pressuredependence.
- Differences between diffusion time constant related to the activation energy.

#### ARTICLE INFO

Article history: Received 2 February 2016 Received in revised form 11 May 2016 Accepted 13 May 2016 Available online 14 May 2016

Keywords: CO<sub>2</sub> diffusion CO<sub>2</sub> adsorption Adsorption kinetics Microporous materials

#### G R A P H I C A L A B S T R A C T



#### ABSTRACT

The equilibrium adsorption and kinetics of  $CO_2$  on several microporous materials has been studied at 273, 283 and 293 K and gas pressures of up to 100 kPa. The porous materials used in this work were two zeolites (5A and 13X), two metal–organic frameworks (Basolite A100 and Basolite Z1200), an activated carbon and two pillared clays (Al-PILC and Zr-PILC). The isothermal and non-isothermal diffusion models were applied to calculate the diffusion time constants ( $D_0/r_c^2$ ) from the uptake curves. The non-isothermal model was found to fit the experimental data well over the whole range of adsorption rates. The values found for the zeolites, which ranged from 0.020 to 0.043 s<sup>-1</sup>, were lower than those for the metal–organic frameworks and pillared clays, which ranged from 0.036 to 0.081 s<sup>-1</sup>, in the same interval of temperatures. Furthermore, the values of the diffusion time constants were found to depend on gas pressure. The pressure-dependence of the diffusion time constants was studied using the Darken equation. Finally, activation energy values were estimated from the temperature-dependence for all materials and it was found to increase in the order: Z1200 < Al-PILC < 13X < AC < Zr-PILC < 5A; A100.

© 2016 Elsevier B.V. All rights reserved.

#### 1. Introduction

The reduction of carbon dioxide emissions to the atmosphere is one of the most important environmental and scientific challenges as current  $\mathrm{CO}_2$  levels are contributing to global warming and

\* Corresponding author.

E-mail address: andoni@unavarra.es (A. Gil).

anthropogenic climate change. The successful use of adsorbents for  $\mathrm{CO}_2$  capture, storage and utilization or for separating  $\mathrm{CO}_2$  from other pollutant gases has been discussed in great detail in several recent reviews [1–4]. The solids considered as adsorbents for  $\mathrm{CO}_2$  capture include zeolites [5], activated carbons [5,6], functionalized mesoporous silica [7], hydrotalcites [8,9], metal–organic frameworks (MOFs) [10–12] and microporous polymers [13].

b Laboratorio de Sólidos Porosos, INFAP, CONICET-Universidad Nacional de San Luis, Chacabuco, 917, 5700 San Luis, Argentina

Table 1 Textural properties derived from  $N_2$  adsorption at 77 K and  $CO_2$  adsorption at 273 K.

Materials	$S_{BET}^{a} (m^2/g)$	Vp <sub>T</sub> <sup>b</sup> (cm <sup>3</sup> / g)	$V\mu p(N_2)^{c} (cm^3/g)$	$V\mu p(CO_2)^d (cm^3/g)$
5A	610	0.31	0.20	0.20
13X	655	0.38	0.22	0.25
A100	465	1.05	0.13	0.57
Z1200	1925	0.77	0.63	0.37
AC	1370	1.12	0.36	0.35
Al-PILC	200	0.12	0.07	0.10
Zr-PILC	310	0.18	0.10	0.10

- <sup>a</sup> Specific surface area calculated using the BET equation.
- <sup>b</sup> Specific total pore volume at a relative pressure of 0.985.
- <sup>c</sup> Specific micropore volume obtained from the  $\alpha_s$ -plot method.
- <sup>d</sup> Specific micropore volume derived from the Dubinin-Radushkevich (DR) equation.

The reliable measurement of adsorption kinetic data is fundamental for the correct design, simulation and development of adsorption/separation processes. A good example of this is the post-combustion capture of CO<sub>2</sub>, in which, if gas diffusion through the pores of the adsorbent is very slow, the time required for each adsorption–desorption cycle is increased, thus resulting in inefficient process rates and greater capture costs. This suggests that intracrystalline CO<sub>2</sub> diffusion rates should be high so as not to be a limiting factor in the overall performance of a CO<sub>2</sub> capture process [14]. These data can be used as parameters in the selection of adsorbents for gas storage, separation and purification [15], and also in heterogeneous catalysis.

The mass transfer mechanism inside adsorbent particles may be controlled by micropore diffusion and/or surface diffusion. Prasetyo and Do [16] studied the adsorption of CO<sub>2</sub> on activated carbon pellets using a semi-batch constant molar flow rate method at 293, 303 and 323 K and low pressures. Analysis of the experimental data obtained at various particle sizes established that adsorption was controlled by both pore- and surface-diffusion mechanisms and a dual model was suggested for the apparent diffusivity calculations. The surface diffusion of hydrocarbons in microporous activated carbon was studied by Do et al. [17,18], and the diffusion of CO<sub>2</sub> on activated carbon beads by Shen et al. [19] in the temperature range 303-423 K and at 0-100 kPa in diluted breakthrough experiments. In this case, micropore resistance controlled the diffusion mechanism. Metal-organic frameworks (MOFs) are potentially useful in several separation applications. Chmelik et al. [20] used infra-red-microscopy (IRM) experiments to determine the diffusivities of CO2 and CH4 in binary mixtures along with those of the individual pure components in a single MOF crystal at 298 K. The effective Fick diffusivities were calculated by fitting the isothermal model to the uptake rates. Considering other materials with a two-dimensional structure, and to the best of our knowledge, there are no data in the literature on CO2 diffusion in pillared clays [21] under the experimental conditions studied in this work. In the current work a study of the adsorption of CO<sub>2</sub> on various microporous materials is carried out under the same conditions, in order to compare the results and to find the mechanism that controls in each case the diffusion process.

A study of the sorbate concentration or pressure-dependence of diffusion is important when it comes to understanding the mechanism of diffusion processes and to developing models for such processes [22]. A strong dependency of surface diffusivity on pressure and concentration has been revealed [18], and other studies have shown a slight dependence of intracrystalline diffusivity at very low pressures. Although the Darken equation has traditionally been extensively used due to its ability to correctly predict experimental data in the low pressure range, it is unable to describe a strong pressure-dependence, especially at high pressures. Another

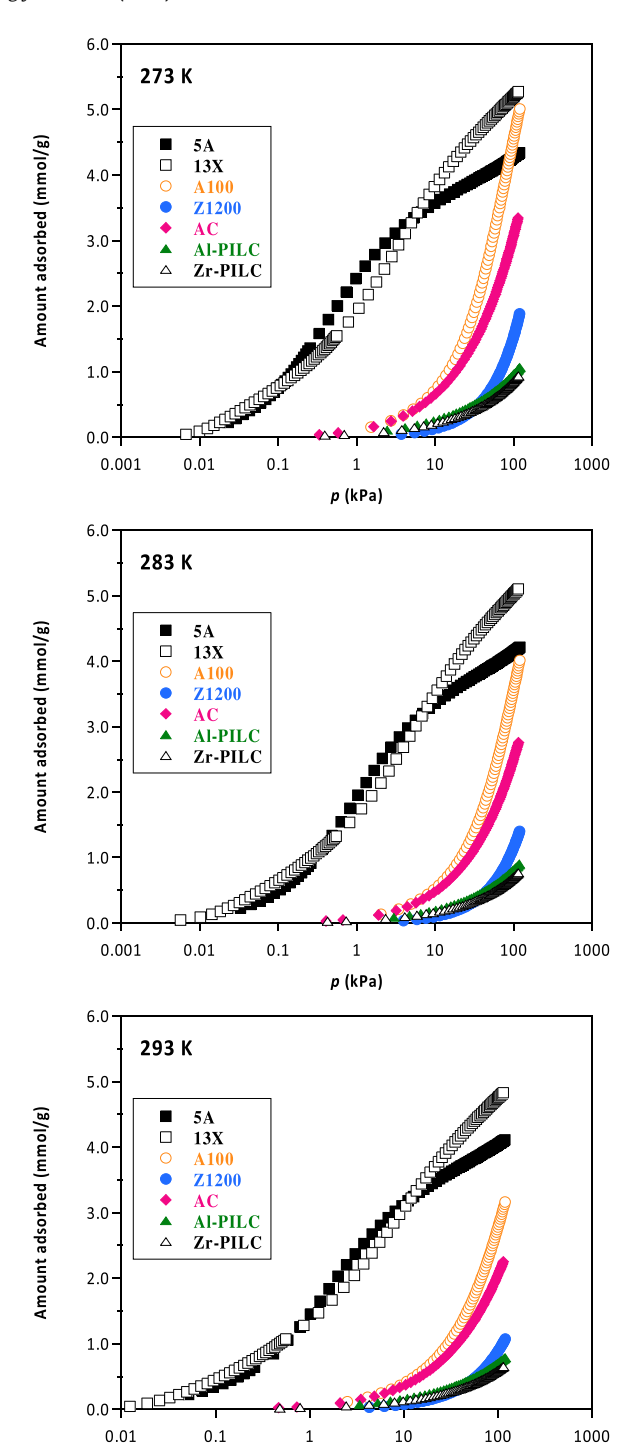


**Fig. 1.** Semi-logarithmic plot of the CO<sub>2</sub> adsorption at 273, 283 and 293 K on the microporous materials. ( $\blacksquare$ ) 5A, ( $\square$ ) 13X, ( $\bigcirc$ ) A100, ( $\bullet$ ) Z1200, ( $\bullet$ ) AC, ( $\blacktriangle$ ) Al-PILC and ( $\triangle$ ) Zr-PILC.

p (kPa)

approach is the model proposed by Do [17], which takes into account the effect of the structure of the solid on transport surface diffusivity. This study found that, in combination with the Toth isotherm, the structural model proposed provides a good prediction of the sorption rate of various molecules on activated carbon when measured in the low-pressure range. Bae and Lee [23] also used the structural model to explain the pressure-dependence of CO<sub>2</sub>, CH<sub>4</sub>, O<sub>2</sub> and N<sub>2</sub> diffusion on carbon molecular sieves at low and high pressures, and these authors also proposed a supercritical

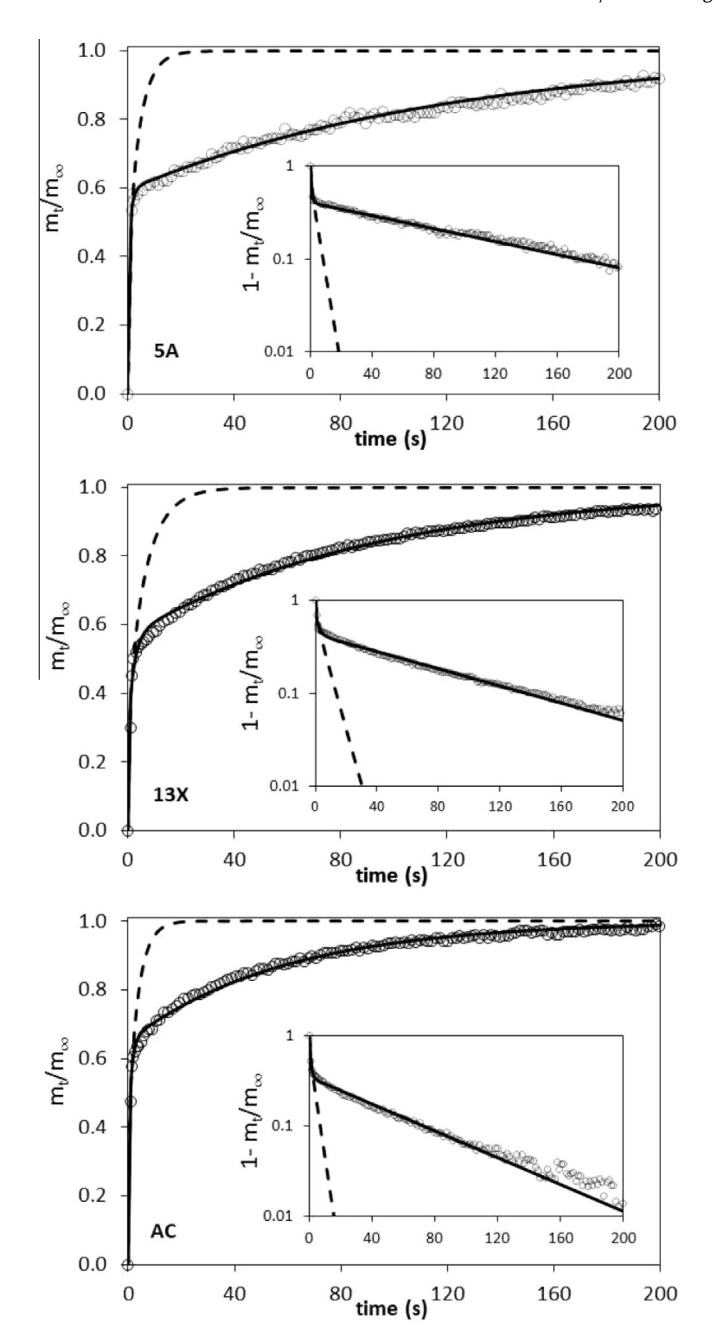


**Fig. 2.** Fractional uptake curves shown on both a lineal and a semi-logarithmic scale for equilibrium pressure at 100 kPa and 293 K for 5A, 13X and AC. (-) Isothermal model fitting, (-) non-isothermal model fitting.

model based on the structural model in order to explain the strong pressure-dependence of the diffusion time constants. This model was found to be more accurate than both the Darken equation and the structural diffusion model, even at low pressures.

The main goal of this work was therefore to undertake a systematic study of the adsorption kinetics of CO<sub>2</sub> on several representative microporous materials such as: two zeolites (5A and 13X), two MOFs (Basolite A100 and Basolite Z1200), an activated carbon (Darko-KB-B), and two pillared clays (Al-PILC and Zr-PILC) at 273, 283 and 293 K and pressures ranging from approximately 14–100 kPa. The diffusion time constants were estimated from the experimental uptake-curves using the isothermal and non-isothermal sorption kinetics models. Additionally, a model was used to investigate the dependence of gas diffusivity on pressure.

The temperature-dependence of the diffusion time constants was also estimated and reported. The information included in this work, such as the comparison of the diffusion time constants for the materials, is currently not available in the open literature for some of these solids.

#### 2. Experimental section

#### 2.1. Materials

The porous solids used in this work included two zeolites (5A (Fluka) and 13X (Sigma–Aldrich)), two MOFs (Basolite A100 (MIL-53-Al) and Basolite Z1200 (ZIF-8) purchased from Sigma–Aldrich), an activated carbon (AC; Sigma–Aldrich, Darko KB-B), and two synthetic pillared clays (Al-PILC and Zr-PILC). The characteristics and properties of the materials selected in this study have been described previously [24–27].

#### 2.2. Adsorption experiments

Nitrogen (Air Liquide, 99.999%) adsorption experiments at 77 K were performed using a static volumetric apparatus (Quantachrome Autosorb-iQ). Carbon dioxide (Air Liquide, 99.998%) adsorption measurements at 273, 283 and 293 K and gas pressures of up to 100 kPa were performed using a Micromeritics ASAP 2010 adsorption analyzer under equilibrium and kinetic conditions. The adsorption temperature was kept constant using a circulating thermostatic bath (Polyscience, model 9702) containing Dynalene HC-50 as the heat-transfer medium. The materials were placed in a sample holder and immersed in a dewar containing the same liquid for accurate temperature control. All samples (0.2 g) were previously degassed under vacuum (pressure lower than 0.133 Pa) for 24 h at 473 K. High-resolution CO<sub>2</sub> adsorption measurements were conducted at low temperatures, chosen in light of literature reports [28] that piezometric methods present limitations in the case of fast kinetics or strongly adsorbed species, thus meaning that a lower temperature (i.e. slower kinetics) provides the appropriate conditions for a reliable determination of diffusivity. The kinetic study was made in the experiments in which the equilibrium isotherms were obtained. For the adsorption kinetic measurements, small stepwise changes in the adsorbate gas pressure with time were recorded and converted into transient adsorption amounts as a function of time, thus giving the adsorption uptake curves.

## 3. Theory. Adsorption kinetics

The rate of gas adsorption on microporous solids can be measured from volumetric experiments by determining the amount adsorbed as a function of time (uptake curve). These experimental data, together with models for gas adsorption in microporous solids, can be used to obtain diffusion time constants, which indicate how easily the adsorbate diffuses into the micropores of the adsorbent. Since adsorption is an exothermic process and the heat of sorption must be dissipated by heat transfer, there is usually a temperature difference between the particle and the surrounding fluid. Whether or not this temperature difference is significant depends on the rates of mass and heat transfer. If heat transfer resistance can be neglected, the system can be treated as isothermal; otherwise, a non-isothermal behavior must be considered [30]. Both isothermal and non-isothermal diffusion models have been used to calculate the diffusion time constants from the uptake curves [29,30].

The isothermal model assumes that the surface barriers, temperature change of the adsorbent and heat transfer between the particle and the surrounding fluid are negligible during the adsorp-

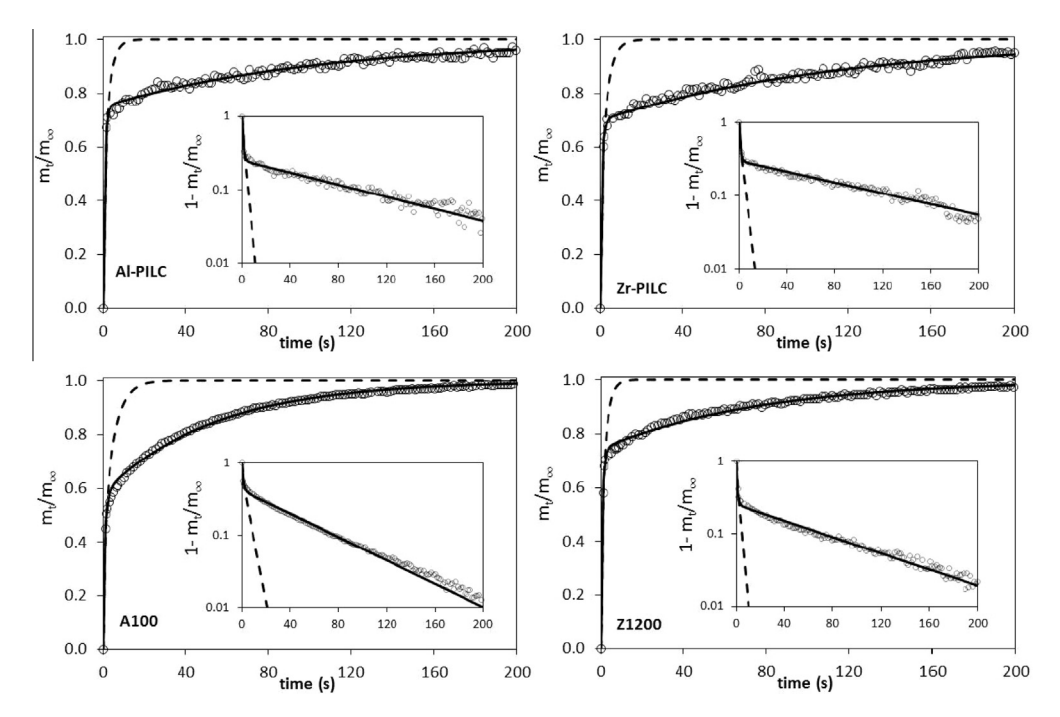


**Fig. 3.** Fractional uptake curves shown on both a lineal and a semi-logarithmic scale for equilibrium pressure at 100 kPa and 293 K for Al-PILC, Zr-PILC, A100 and Z1200 materials. (—) Isothermal model fitting, (—) non-isothermal model fitting.

tion process. For most particle shapes, representation as an equivalent sphere is an acceptable approximation with little numerical difference from the response for other particle shapes [31]. The isothermal model is a valid approximation when diffusion is slow compared with heat transfer [18,30]. When the uptake of gas by the adsorbent is small relative to the total amount of gas in the system, the ambient sorbate concentration remains practically constant after the initial small step change. The solution for the uptake curve is given by Eq. (1) [30]:

$$\frac{q(t) - q_0}{q_{\infty} - q_0} = \frac{m_t}{m_{\infty}} = 1 - \frac{6}{\pi^2} \sum_{n=1}^{\infty} \frac{1}{n^2} \exp\left(-n^2 \pi^2 \left(\frac{D_c}{r_c^2}\right) t\right)$$
(1)

where  $m_t/m_\infty$ , is the fractional approach to equilibrium (also known as fractional uptake);  $q_0$ , q(t) and  $q_\infty$  are the initial amount adsorbed (mmol/g) and the amounts adsorbed at time t and at equilibrium, respectively;  $D_c$  (cm²/s) is the apparent diffusivity of gas molecules in porous media;  $r_c$  (cm) is the crystal radius; and t (s) is the time. The ratio  $D_c/r_c^2$  (s<sup>-1</sup>) is known as the diffusion time constant.

The non-isothermal diffusion model is useful for analyzing experimental uptake curves for rapidly diffusing systems in which sorption kinetics are mainly dominated by thermal effects [29,32–34]. The main assumptions are the same as in the case of the isothermal model, with the important difference that the heat transfer resistance is taken into account. The rate-limiting step is the heat transfer between the particle and the gas film which surrounds it, rather than the conduction of heat within the particle. The expressions for the uptake curves are given by the following equations [29,32]:

$$\frac{m_t}{m_{\infty}} = 1 - \sum_{n=1}^{\infty} \frac{9 \left[ (q_n \cot(q_n) - 1) / q_n^2 \right]^2 \exp\left( -q_n^2 \frac{D_t}{r_t^2} t \right)}{\frac{1}{\theta} + \frac{3}{2} \left[ q_n \cot(q_n) (q_n \cot(q_n) - 1) / q_n^2 + 1 \right]}$$
(2)

The values of  $q_n$  are the roots of the following equation [29,32]:

$$3\beta(q_n\cot(q_n) - 1) = q_n^2 - \alpha \tag{3}$$

The dimensionless parameters  $\alpha$  and  $\beta$  are related to the heat-transfer process according to Eqs. (4) and (5):

$$\alpha = \frac{\text{ha}}{\rho C_p} \frac{r_c^2}{D_c} \tag{4}$$

$$\beta = \frac{\Delta H}{C_p} \left( \frac{\partial q^*}{\partial T} \right)_p \tag{5}$$

where h (cal/cm<sup>2</sup> s K), a (1/cm),  $\rho$  (g/cm<sup>3</sup>) and  $C_p$  (cal/g K) are the heat-transfer coefficient, the surface-to-volume ratio, the density and the heat capacity of the adsorbent, respectively;  $\Delta H$  (cal/mmol) is the sorption heat; and  $(\partial q^*/\partial T)_p$  corresponds to the equilibrium concentration of the adsorbate as a function of temperature at constant equilibrium pressure. The values of  $\beta$  and  $ha/\rho C_p$  can be calculated directly from the asymptotic part of the uptake curves given by Eq. (6) [29,32]:

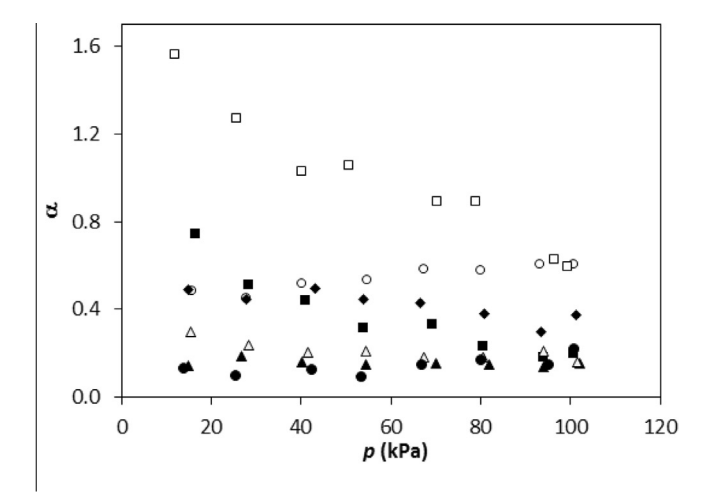
$$\frac{m_t}{m_\infty} = 1 - \frac{\beta}{1+\beta} \exp\left[-\frac{ha}{\rho C_p} \frac{t}{(1+\beta)}\right] \tag{6}$$

The parameters  $\beta$  and ha/ $\rho C_p$  herein are calculated from the slope and intercept of a semi-logarithmic plot of  $1-m_t/m_\infty$  vs. t [29], and the diffusion time constants are extracted iteratively from the above equations.

### 3.1. Pressure-dependence of the diffusion time constant

The Darken equation is the most widely used model to explain the dependence of diffusivity and the diffusion time constant on adsorbate concentration or pressure. Based on the assumption that the chemical potential gradient is the true driving force for diffusion and ideal gas behavior, Darken [35] proposed a relationship between the diffusion of ions in metallic systems in which diffusion and mobility are related to free energy. Sorbate pressure or concentration-dependence is derived from the Darken equation on the basis of the relationship between the true diffusivity and the Fickian diffusivity using the following expression [21,36]:

$$D_{c} = D_{0} \frac{\partial \ln p}{\partial \ln q} \tag{7}$$



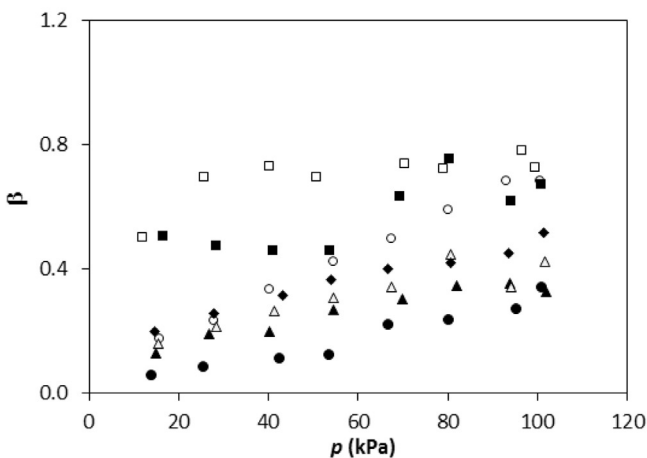


**Fig. 4.** Values of  $\alpha$  and  $\beta$  obtained from non-isothermal analysis of CO<sub>2</sub> sorption curves at 293 K in ( $\blacksquare$ ) 5A, ( $\square$ ) 13X, ( $\bigcirc$ ) A100, ( $\spadesuit$ ) Z1200, ( $\spadesuit$ ) AC, ( $\Delta$ ) Al-PILC and ( $\Delta$ ) Zr-PILC.

where  $D_0$  is the so-called corrected diffusivity or limiting diffusion, which represents the diffusivity at zero loading or pressure, and  $\partial lnp/\partial lnq$  is the thermodynamic correction factor, which is obtained from the adsorption isotherm. When the Langmuir, Toth or Sips equations are used to describe the adsorption equilibrium, the Darken equation, in terms of diffusion time constant, takes the following forms:

$$\frac{D_c}{r_c^2} = \frac{D_0}{r_c^2} (1 + b_L p) \tag{8}$$

$$\frac{D_c}{r_c^2} = \frac{D_0}{r_c^2} \left( 1 + (b_T p)^{n_T} \right) \tag{9}$$

$$\frac{D_c}{r_c^2} = \frac{D_0}{r_c^2} \left( 1 + (b_S p)^{1/n_S} \right) \tag{10}$$

The constant  $D_0/r_c^2$  (s<sup>-1</sup>) was obtained by non-linear regression of  $D_c/r_c^2$  vs. p.

### 3.2. Temperature-dependence of the diffusion time constant

The dependence of diffusion time constants can be described by an Arrhenius-type equation:

$$\frac{D_c}{r_c^2} = \frac{D_\infty}{r_c^2} \exp\left(-\frac{E_a}{RT}\right) \tag{11}$$

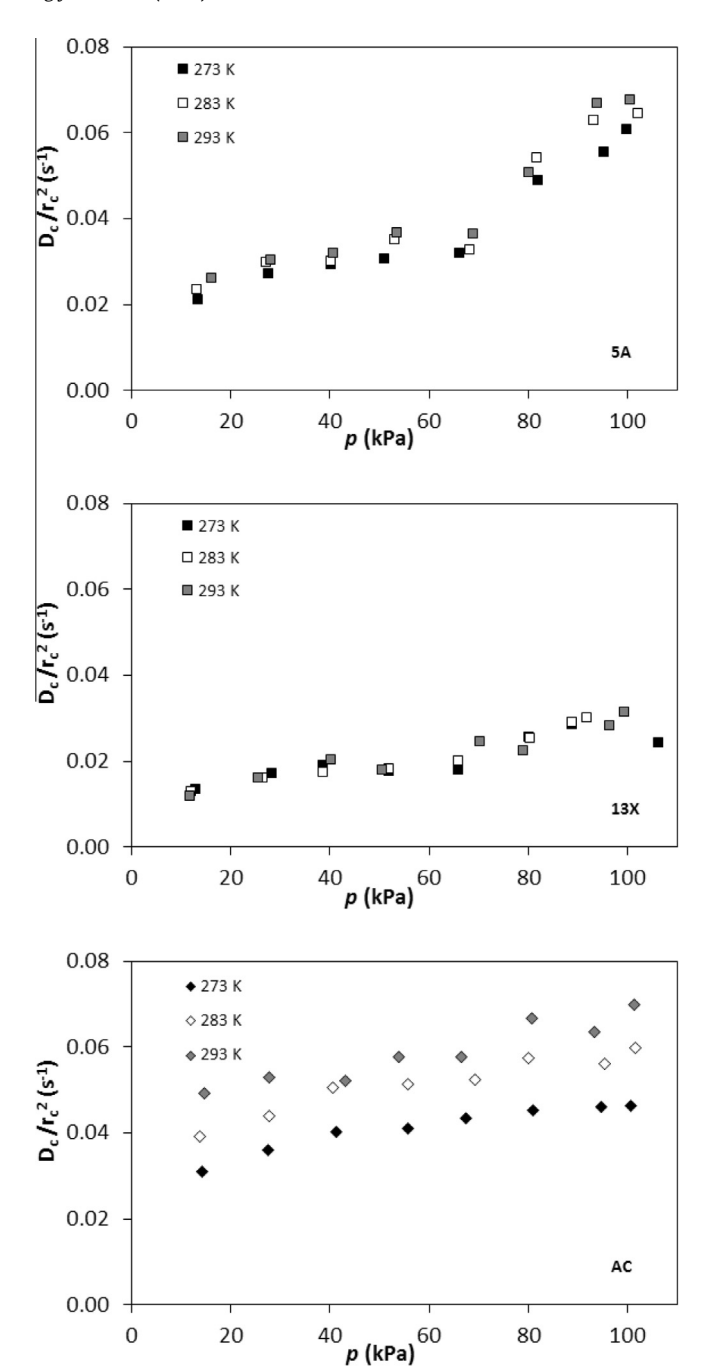


Fig. 5. Pressure-dependence models of the diffusion time constants for  $CO_2$  at 273, 283 and 293 K and pressures up to 100 kPa for 5A, 13X and AC.

where  $D_{\infty}/r_c^2$  and  $E_a$  are the pre-exponential factor and the activation energy for diffusion, respectively. This equation of dependence can also be provided with the limiting diffusion time constant  $D_0/r_c^2$ . The magnitude of  $E_a$  reflects the energetic barriers that the molecules have to overcome on their diffusion path in the intracrystalline space [37].

#### 4. Results and discussion

The characterization of adsorbent materials and the assessment of their suitability for a given application require the determination of the equilibrium and kinetic behaviour of the solids. The main textural properties of all materials used in this work are sum-

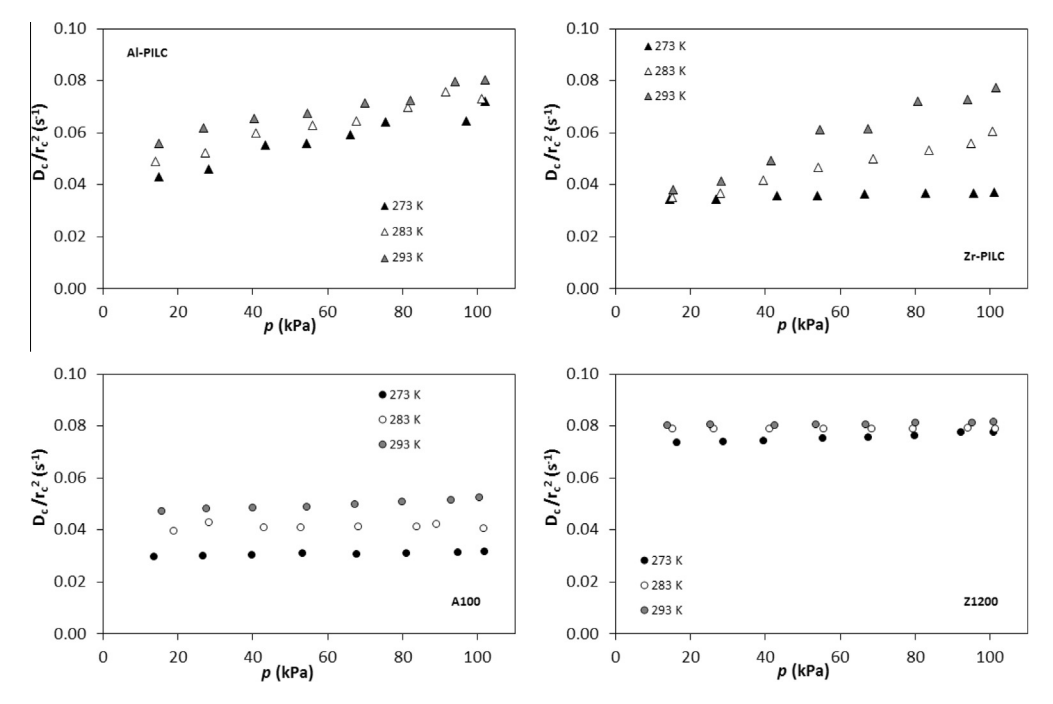


Fig. 6. Pressure-dependence models of the diffusion time constants for CO2 at 273, 283 and 293 K and pressures up to 100 kPa for Al-PILC, Zr-PILC, A100 and Z1200.

**Table 2** Average values of diffusion time constants  $(D_c/r_c^2)$  estimated using the non-isothermal model (Eq. (2)) at 273, 283 and 293 K in the pressure range up to 100 kPa.

	$D_c/r_c^2 (s^{-1}) \times 10^{-2}$			
	273 K	283 K	293 K	
5A	3.797	4.146	4.316	
13X	2.028	2.095	2.141	
AC	4.118	5.14	5.87	
Al-PILC	5.75	6.33	6.94	
Zr-PILC	3.591	4.743	5.92	
A100	3.055	4.096	4.94	
Z1200	7.53	7.87	8.06	

marized in Table 1. The specific surface areas ( $S_{BET}$ ) were estimated using the Brunauer, Emmett and Teller (BET) equation [38] according to the criteria suggested by Rouquerol et al. [39]. The total pore volume (Vp<sub>T</sub>) was calculated from the amount of nitrogen adsorbed at a relative pressure of 0.985 assuming that the density of the nitrogen condensed in the pores is equal to that of liquid nitrogen at 77 K [40]. The micropore volumes ( $V\mu p(N_2)$ ) were calculated using the  $\alpha_S$ -plot method [38], with nonporous hydroxylated silica as the reference adsorbent [41] for 5A, 13X, A100 and Z1200, nonmicroporous PILC materials as reference adsorbents [21] for Al-PILC and Zr-PILC, and the nonmicroporous activated carbon CarbonA as reference adsorbent [42] for the AC material. The micropore volumes  $(V\mu p(CO_2))$  were also calculated using the Dubinin-Radushkevich equation [43] over the relative pressure range 0.01–0.034 for carbon dioxide adsorption at 273 K. The  $V\mu p$  $(N_2)$  values for the samples give the order Z1200 > AC > 13X > 5A > A100 > Zr-PILC > Al-PILC, and the  $V\mu p(CO_2)$  values yield the order A100 > Z1200 > AC > 13X > 5A > Zr- and Al-PILC. A100, for which  $V\mu p(N_2) < V\mu p(CO_2)$ , exhibits a narrow microporosity that cannot be measured by N<sub>2</sub> adsorption, whereas Z1200 presents large micropores  $(V\mu p(N_2) > V\mu p(CO_2))$ . In general, the MOF materials present the largest micropore volumes and the PILC samples the smallest due to the structure of the materials.

The CO<sub>2</sub> adsorption equilibrium isotherms determined at 273, 283 and 293 K and pressures of up to 100 kPa are presented in

Fig. 1 for all seven adsorbents studied. It can readily be seen that the zeolite samples have the strongest affinity for CO<sub>2</sub>, with these isotherms showing the highest saturation loading, whereas a maximum loading cannot be reached for the other materials under the experimental conditions used herein. The behavior of the CO<sub>2</sub> adsorption isotherm for zeolite 5A at 273 K is in accordance with those reported in the literature [44,45]. In the case of PILCs, the lower adsorption capacity of CO<sub>2</sub> is probably influenced by the specific surface area, the porosity, the pore volume, as well as physical interactions with CO<sub>2</sub> molecules [46,47], as evidenced by the lower surface areas and pore volumes obtained for the Aland Zr-PILC samples. All equilibrium data were predicted using the Langmuir. Toth and Sips equations, and the fitting parameters are summarized in Table S1 in the Supporting Information. The results suggest that the Toth and Sips equations fit the CO2 adsorption isotherms better than the Langmuir equation.

The uptake curves obtained from volumetric experiments reflect transport of the gas into, or out of, the pores of the adsorbent upon increasing the pressure [48]. Representative experimental fractional uptake curves vs. time for the microporous materials at 293 K and pressures of 100 kPa, as well as the corresponding fitting with the isothermal (Eq. (1)) and non-isothermal (Eq. (2)) models, are presented in Figs. 2 and 3. It can be seen from these results that the isothermal model is unable to describe the whole experimental curve. Many studies have reported a similar kinetic behavior for several sorbates on zeolites [30,44,48] and carbonaceous materials [49], with strong adsorption and pronounced heat effects resulting in significant deviations from the values predicted by the isothermal model. In those cases in which significant effects are seen, the non-isothermal model has been suggested to be suitable for correct interpretation of the experimental data. Consequently, the non-isothermal model was used to obtain the diffusion time constants in the range of pressures up to about 100 kPa in this work.

In the non-isothermal model, for either  $\alpha \to \infty$  (in Eq. (4), infinitely high heat transfer coefficient) or  $\beta \to 0$  (in Eq. (5), infinitely large heat capacity or heat of adsorption) the limiting case is the isothermal behavior, and complete heat control is observed in

those cases where the value of  $\alpha$  is small. The values of  $\alpha$  and  $\beta$  at 293 K calculated in this work are shown in Fig. 4, and the full results at the three temperatures studied are provided in Figs. S1 and S2 in the Supporting Information. It can be seen that the values of  $\alpha$  decrease slightly with increasing pressure in some cases, thereby possibly indicating that non-isothermal behavior becomes pronounced at high pressures. In the case of A100 and Al-PILC, the values of  $\alpha$  remain constant over the whole pressure range. As regards the values of  $\beta$ , PILCs and Z1200 exhibited lower values than zeolites and A100, the  $\beta$  values for which were higher. This behavior can be associated with the heats of CO<sub>2</sub> adsorption of these materials, which follow a similar trend in terms of isosteric heats [24].

The diffusion time constants  $D_c/r_c^2$ , as determined from the fractional uptake curves for pressures of between 14 and 100 kPa at 273, 283 and 293 K and applying Equation (2), are represented graphically in Figs. 5 and 6. In order to allow a comparison between the seven materials, average  $D_c/r_c^2$  values were calculated for the aforementioned pressure range for each temperature and material studied. These results are summarized in Table 2.

Many factors could influence the diffusion behavior in each type of zeolite. It has long been known that the size of the diffusing molecules relative to the pore opening of zeolites (window aperture size) is an important factor that affects the diffusional resistance [50,51], although the interaction between the cation in the cages of zeolites and the adsorbate molecules also plays an important role [51]. In this work we found that the diffusion time constant of CO2 is smaller in 13X than in 5A. Taking into account that the kinetic diameter of the CO<sub>2</sub> molecule (0.33 nm) is considerably smaller than the pore diameter of the zeolites (0.5 nm for 5A and 0.74 nm for 13X) [24], it can be suggested that the main differences between the two zeolites studied arise due to the different interaction of CO<sub>2</sub> with the cations present in them (calcium for 5A and sodium for 13X) and the pore structure of each zeolite. A similar behavior was reported previously in the literature [51]. In addition, according to Ruthven [50], the distribution of the cations in the zeolite framework can lead to pore blocking or facilitate the passage of the molecule through the window. The diffusion time constant for CO<sub>2</sub> in 5A is of the same order of magnitude as those reported in the literature [32], as are the  $D_c/r_c^2$  values obtained for 5A and 13X using the isothermal model [45,52]. Furthermore, the highest values for CO<sub>2</sub> diffusion were found in PILCs and Z1200, and an analysis of the adsorption isotherm confirms that these adsorbents possess larger micropore sizes than zeolites, thus allowing faster diffusion. In the case of the PILCs, the pore structure of the clays, intermolecular interactions, the size of the sorbent molecules and the strength of adsorption on the surface of pillars can all influence the diffusion [53]. The movement of molecules in the complex structure of pillared clays is limited to a pore space that has to be able to connect one layer to another, and access to the internal pore volume is controlled by the distance between silicate layers and the interpillar distance [54]. According to this, a comparison of the two pillared clays gives pore sizes in the order

Zr-PILC < Al-PILC. Moreover, as these values are smaller than the free interlayer distances [25], the fact that the diffusion time constants of  $\mathrm{CO}_2$  are smaller in Zr-PILC than in Al-PILC must be related to the smaller pore size. The Zr pillaring increases the NH<sub>3</sub> adsorption capacity [55], but this capacity appears to not be proportionally related to the diffusion time constant so the effect must be due to the developed porous structure.

As regards the diffusion time constants for the two MOFs, the higher values found for the Z1200 material can be explained in terms of pore structure and the strength of its electrostatic interactions with CO<sub>2</sub>. In relation to the pore network of these materials, Z1200 has internal cavities with a pore diameter of 1.16 nm and a window aperture of 0.34 nm [24]. Consequently, given the similarity in size between the kinetic diameter of CO<sub>2</sub> and this aperture, it is expected that the rate limiting factor will be the aperture size. However, several studies [56.57] have reported that the Z1200 framework structure is, in fact, more flexible, thus allowing fast diffusion through the window. As such, it seems that the diffusion of CO<sub>2</sub> molecules through the Z1200 framework structure is directly influenced by the cavity size (1.16 nm). In the case of A100, this MOF consists of a single pore size of 0.85 nm, which is considerably smaller than the cavity size of Z1200, thereby resulting in a lower diffusion time constant than for the Z1200 material.

Furthermore, frameworks containing coordinately unsaturated metal sites can selectively interact with  $CO_2$  molecules [10]. In the case of A100, these interactions are stronger than in Z1200, as evidenced by the higher isosteric heat of adsorption in A100 compared with that in Z1200, 28.60 and 19.56 kJ/mol, respectively [24]. This fact suggests that  $CO_2$  is less strongly adsorbed, thus meaning that it can pass into Z1200 windows and cages much faster.

The diffusion time constant values obtained for the AC are found between those obtained for zeolites (lower values) and Z1200 (higher values) and are explained in terms of their pore size distribution. It is well known that molecular sieves have well-defined and narrow pore sizes, thus leading to slower diffusion than in MOFs. In order to determine the pore size distribution (PSD) of the activated carbon used in this work, a non-local density functional theory (NLDFT) method was implemented using the CO<sub>2</sub> adsorption isotherm with the kernel for CO<sub>2</sub> at 273 K on a carbon surface with the slit pore model, which is applicable to pore sizes ranging from 0.35 to 1.5 nm [58]. This result is included in Fig. S3 in the Supporting Information. It can readily be seen that AC has pore sizes distributed throughout the whole range of micropores, and this heterogeneous porosity lies between the porosity of zeolites and Z1200.

The diffusion time constants for zeolites, PILCs and AC revealed a slight pressure-dependence, increasing with pressure (see Figs. 5 and 6). At very low pressures, adsorption occurs in the smallest pores, or ultramicropores (most energetic sites), whereas as the pressure increases the sorption rate is relatively fast as adsorption occurs at the larger pores, which have a relatively low energy barrier (higher mobility) [18,23]. In recent studies [45,59,60], in which

**Table 3**Pressure-dependence obtained using the Darken–Toth model and its parameters at 273, 283 and 293 K.

	T = 273 K		T = 283 K		T = 293 K				
	$D_0/r_c^2 (s^{-1})$	$b_i$ (kPa $^{-1}$ )	$n_i$	$D_0/r_c^2 (s^{-1})$	$b_i$ (kPa $^{-1}$ )	$n_i$	$D_0/r_c^2 (s^{-1})$	$b_i$ (kPa $^{-1}$ )	$n_i$
5A	1.740E-03	4.291	0.556	2.456E-03	2.100	0.581	3.310E-03	1.137	0.598
13X	2.364E-03	4.853	0.3647	2.991E-03	4.278	0.3354	3.593E-03	2.316	0.3370
AC	2.673E-02	4.400E-03	0.4300	3.570E-02	3.600E-03	0.5100	4.295E-02	3.700E-03	0.630
Al-PILC	3.280E-02	5.00E-03	0.2050	3.879E-02	1.445E-03	0.1738	4.243E-02	2.800E-03	0.3100
Zr-PILC	2.191E-02	1.699E-03	0.1875	3.017E-02	8.08E-04	0.1729	4.077E-02	3.396E-04	0.1924
A100	2.131E-02	7.89E-03	1.306	3.240E-02	3.295E-03	0.838	4.105E-02	3.986E-04	0.4164
Z1200	7.53E-02	1.551E-04	2.365	7.87E-02	1.182E-04	2.365	8.06E-02	8.75E-05	16.799

**Table 4** Activation energies for diffusion of CO<sub>2</sub> in microporous materials.

	$E_a$ (kJ/mol)	$E_a$ (Literature) (kJ/mol)
5A	21.4	28.9 [51]; 29.7 [61]
13X	13.9	10 [37]; 35.6 [51]; 1.8 [52]; 11.7 [61]
AC	15.8	13.8 [16]; 18.1 [19]
Al-PILC	8.59	
Zr-PILC	20.6	
A100	21.9	
Z1200	2.27	

micropore diffusion constants for  $\mathrm{CO}_2$  in microporous materials were obtained, the increasing trend in diffusion time constants was attributed to surface diffusion and the dominant interaction between sorbate molecules and pore walls. Similarly, Do [17] suggested that the fast increase of diffusivity in activated carbons is due to the presence of disordered regions between the graphitic units and the penetration of molecules from the gas phase into these units (micropores). In the case of MOF materials, the diffusion time constants showed a weak pressure-dependence.

The pressure-dependence of the diffusion time constants was estimated using the Darken equation in combination with the Langmuir, Toth and Sips isotherm equations (Eqs. from (8)–(10)). The values of the fit parameter  $D_0/r_c^2$  obtained from the Darken–Toth equation (Eq. (9)) are summarized in Table 3. The complete results of fitting are provided in Table S2 in the Supporting Information.

Intracrystalline diffusion is an activated process. In the case of zeolites, Ruthven [50] has pointed out that low diffusion activation energy values are obtained from the temperature-dependence of the Fickian diffusivity at a fixed partial pressure, or outside Henry's law. This author suggests that the activation energy should be calculated from the corrected diffusivities  $D_0$  or  $D_0/r_c^2$ . The Arrhenius equation was used to gain some idea of the temperaturedependence of the diffusion time constant data obtained in this work. In accordance with the procedure described by Ruthven, the values of  $D_0/r_c^2$  obtained from the Darken-Toth equation were used to estimate the activation energy,  $E_a$ , for all materials, from the lineal form of the Arrhenius expression ( $\ln D_0/r_c^2$  vs. 1/T). The Toth model was selected because it is a well-known isotherm equation developed for heterogeneous materials, presents a correct behavior over the entire pressure range and is a relatively simple model that can effectively describe many systems. The results are shown in Table 4. The reported literature data for AC and zeolites 5A and 13X are also included in Table 4. Our activation energy values are in agreement with those found in the literature [16,19,37,51,61]. In general, the activation energy values are influenced by factors such as pore width, location of the cation in the diffusion path and the interaction between the diffusing species and the adsorbent. In this regard, the interaction of the permanent electrostatic quadrupole moment of the CO<sub>2</sub> molecule with the accessible cations in the materials could influence the energy barriers that control microporous diffusion.

#### 5. Summary and conclusions

This work has presented a quantitative study and a comparison of the diffusion time constants of  ${\rm CO_2}$  on seven microporous materials at 273, 283 and 293 K and gas pressures of up to 100 kPa. Adsorption isotherm and diffusion time constants have been calculated from the measured uptake rates.

The isothermal and non-isothermal diffusion models have been evaluated and used to calculate the diffusion time constants from the uptake curves. Good predictions were obtained using the non-isothermal diffusion model. It was found that the diffusion

time constants increase in the following order: 13X < 5A; A100 < AC < Zr-PILC < Al-PILC < Z1200. The lowest  $CO_2$  diffusion values are obtained for zeolites, with the highest values being found for Z1200 and PILCs.

The Darken equation has been used to study the pressure-dependence of the diffusion time constants using the Langmuir, Toth and Sips isotherm equations. The Darken equation provided a good prediction of the diffusion time constant for all materials. With regard to the temperature-dependence of the diffusion time constants, activation energy values were estimated, and a comparison of the  $E_0$  values for the seven materials gave the following order: Z1200 < Al-PILC < 13X < AC < Zr-PILC < 5A; A100.

# Acknowledgements

This work was supported by the Spanish Ministry of Economy and Competitiveness (*MINECO*) through the project PRI-PIBAR-2011-1369. S.I. Garcés-Polo acknowledges financial support from the Public University of Navarra through a PhD fellowship.

#### Appendix A. Supplementary data

Supplementary data associated with this article can be found, in the online version, at http://dx.doi.org/10.1016/j.cej.2016.05.057.

#### References

- D.M. D'Alessandro, B. Smith, J.R. Long, Carbon dioxide capture: prospects for new materials, Angew. Chem. Int. Ed. 49 (2010) 6058–6082.
- [2] S. Choi, J.H. Drese, C.W. Jones, Adsorbents materials for carbon dioxide capture from large anthropogenic point sources, ChemSusChem 2 (2009) 796–854.
- [3] J. Wang, L. Huang, R. Yang, Z. Zhang, J. Wu, Y. Gao, Q. Wang, D. O'Hare, Z. Zhong, Recent advances in solid sorbents for CO<sub>2</sub> capture and new development trend, Energy Environ. Sci. 7 (2014) 3478–3518.
- [4] B.P. Spigarelli, S. Komar Kawatra, Opportunities and challenges in carbon dioxide capture, J. CO2 Util. 1 (2013) 69–87.
- [5] K.T. Chue, J.N. Kim, Y.J. Yoo, S.H. Cho, R.T. Yang, Comparison of activated carbon and zeolites 13X for CO<sub>2</sub> recovery from flue gas by pressure swing adsorption, Ind. Eng. Chem. Res. 34 (1995) 591–598.
- [6] E.S. Kikkinides, R.T. Yang, Concentration and recovery of CO<sub>2</sub> from flue gas by pressure swing adsorption, Ind. Eng. Chem. Res. 32 (1993) 2714–2720.
- [7] P.J.E. Harlick, A. Sayari, Applications of pore-expanded mesoporous silicas. 3. Triamine silane grafting for enhanced CO<sub>2</sub> adsorption, Ind. Eng. Chem. Res. 45 (2006) 3248–3255.
- [8] E.L.G. Oliveira, C.A. Grande, A.E. Rodrigues, CO<sub>2</sub> sorption on hydrotalcite and alkali-modified (K and Cs) hydrotalcites at high temperature, Sep. Purif. Technol. 62 (2008) 137–147.
- [9] C.V. Miguel, R. Trujillano, V. Rives, M.A. Vicente, A.F.P. Ferreira, A.E. Rodrigues, A. Mendes, L.M. Madeira, High temperature CO<sub>2</sub> sorption with galliumsubstituted and promoted hydrotalcites, Sep. Purif. Technol. 127 (2014) 202– 211.
- [10] P.D.C. Dietzel, V. Besikiotis, R. Blom, Application of metal-organic frameworks with coordinatively unsaturated metal sites in storage and separation of methane and carbon dioxide, J. Mater. Chem. 19 (2009) 7362–7370.
- [11] J.-R. Li, Y. Ma, M.C. McCarthy, J. Sculley, J. Yu, H.-K. Jeong, P.B. Balbuena, H.-C. Zhou, Carbon dioxide capture-related gas adsorption and separation in metalorganic frameworks, Coord. Chem. Rev. 255 (2011) 1791–1823.
- [12] K. Sumida, D.L. Rogow, J.A. Mason, T.M. McDonald, E.D. Bloch, Z.R. Herm, T.-H. Bae, J.R. Long, Carbon dioxide capture in metal-organic frameworks, Chem. Rev. 112 (2012) 724-781
- [13] Ch. Xu, N. Hedin, Microporous adsorbents for CO<sub>2</sub> capture a case for microporous polymers?, Mater Today 17 (2014) 397–403.
- [14] T.-H. Bae, M.R. Hudson, J.A. Mason, W.L. Queen, J.J. Dutton, K. Sumida, K.J. Micklash, S.S. Kaye, C.M. Brown, J.R. Long, Evaluation of cation-exchanged zeolite adsorbents for post-combustion carbon dioxide capture, Energy Environ. Sci. 6 (2013) 128–138.
- [15] D.G. Hartzog, S. Sircar, Adsorption: sensitivity of PSA process performance to input variables, Adsorption 1 (1995) 133–151.
- [16] I. Prasetyo, D.D. Do, Adsorption rate of methane and carbon dioxide on activated carbon by the semi-batch constant molar flow rate method, Chem. Eng. Sci. 53 (1998) 3459–3467.
- [17] D.D. Do, A model for surface diffusion of ethane and propane in activated carbon, Chem. Eng. Sci. 51 (1996) 4145–4158.
- [18] H.D. Do, D.D. Do, I. Prasetyo, On the surface diffusion of hydrocarbons in microporous activated carbon, Chem. Eng. Sci. 56 (2001) 4351–4368.
- [19] C. Shen, C.A. Grande, P. Li, J. Yu, A.E. Rodrigues, Adsorption equilibria and kinetics of CO<sub>2</sub> and N<sub>2</sub> on activated carbon beads, Chem. Eng. J. 160 (2010) 398–407.

- [20] C. Chmelik, J. Van Baten, R. Krishna, Hindering effects in diffusion of CO<sub>2</sub>/CH<sub>4</sub> mixtures in ZIF-8 crystals, J. Membr. Sci. 397–398 (2012) 87–91.
- [21] A. Gil, S.A. Korili, M.A. Vicente, Recent advances in the control and characterization of the porous structure of pillared clay catalysts, Catal. Rev. Sci. Eng. 50 (2008) 153–221.
- [22] R.T. Yang, Gas Separation by Adsorption Processes, Imperial College Press, London, 1997.
- [23] Y.-S. Bae, C.-H. Lee, Sorption kinetics of eight gases on a carbon molecular sieve at elevated pressure, Carbon 43 (2005) 95–107.
- [24] S.I. Garcés, J. Villaroel-Rocha, K. Sapag, S.A. Korili, A. Gil, Comparative study of the adsorption of equilibrium of the CO<sub>2</sub> on microporous commercials materials at low pressures, Ind. Eng. Chem. Res. 52 (2013) 6785–6793.
- [25] A. Gil, F.C.C. Assis, S. Albeniz, S.A. Korili, Removal of dyes from wastewaters by adsorption on pillared clays, Chem. Eng. J. 168 (2011) 1032–1040.
- [26] A.A. García Blanco, A.F. Vallone, A. Gil, K. Sapag, A comparative study of various microporous materials to store hydrogen by physical adsorption, Int. J. Hydrogen Energy 37 (2012) 14870–14880.
- [27] A.A. García Blanco, A.F. Vallone, S.A. Korili, A. Gil, K. Sapag, A comparative study of several microporous materials to store methane by adsorption, Microporous Mesoporous Mater. 224 (2016) 323–331.
- [28] X. Hu, E. Mangano, D. Friedrich, H. Ahn, S. Brandani, Diffusion mechanism of  $CO_2$  in 13 X zeolite beads, Adsorption 20 (2014) 121–135.
- [29] L.K. Lee, D.M. Ruthven, Analysis of thermal effects in adsorption rate measurements, J. Chem. Soc. Faraday Trans. I (75) (1979) 2406–2422.
- [30] D.M. Ruthven, Principles of Adsorption and Adsorption Processes, Jhon Wiley & Sons. New York. 1984.
- [31] D.M. Ruthven, S. Brandani, M. Eic, Measurement of diffusion in microporous solids by macroscopic methods, in: H.G. Karge, J. Weitkamp (Eds.), Adsorption and Diffusion, Molecular Sieves, Science and Technology, 7, 2008, pp. 45–84.
- [32] D.M. Ruthven, L.L.K. Lee, H. Yucel, Kinetics of non-isothermal sorption in molecular sieve crystals, AIChE J. 26 (1980) 16–23.
- [33] H.J. Doelle, L. Riekert, Kinetics of sorption, desorption and diffusion of nbutane in zeolites NaX, ACS Symp. Ser. 40 (1977) 401–417.
- [34] J.D. Eagan, B. Kindl, R.B. Anderson, Kinetic of adsorption on zeolites, Temperature Effect. Molecular Sieve Zeolites II, ACS, Washington, 1971, pp. 164–170.
- [35] L.S. Darken, Diffusion, mobility and their interrelation through free energy in binary metallic systems, Trans. AIME 175 (1948) 184–201.
- [36] D.D. Do, Adsorption Analysis: Equilibria and Kinetics, Imperial College Press, London, 1998.
- [37] J. Kärger, H. Pfeifer, F. Stallmach, N.N. Feoktistova, S.P. Zhdanov, <sup>129</sup>Xe and <sup>13</sup>C PFG n.m.r. study of the intracrystalline self-diffusion of Xe, CO<sub>2</sub>, and CO, Zeolites 13 (1993) 50–55.
- [38] S.J. Gregg, K.S.W. Sing, Adsorption, Surface Area and Porosity, Academic Press, New York, 1991.
- [39] J. Rouquerol, P. Llewellyn, F. Rouquerol, Is the BET equation applicable to microporous adsorbents?, Stud Surf. Sci. Catal. 160 (2007) 49–56.
- [40] F. Rouquerol, J. Rouquerol, K. Sing, Adsorption by Powders and Porous Solids, Academic Press, San Diego, 1999.
- [41] M.R. Bhambhani, P.A. Cutting, K.S.W. Sing, D.H. Turk, Analysis of nitrogen adsorption isotherms on porous and nonporous silicas by the BET and  $\alpha_s$  methods, J. Colloid Interface Sci. 38 (1972) 109–117.

- [42] F. Rodriguez-Reinoso, J.M. Martin-Martinez, C. Prado-Burguete, B. McEnaney, A standard adsorption isotherm of activated carbons, J. Phys. Chem. 91 (1987) 515–516.
- [43] M.M. Dubinin, Fundamentals of the theory of adsorption in micropores of carbon adsorbents: characteristics of their adsorption properties and microporous structures, Carbon 27 (1989) 457–467.
- [44] H. Yucel, D.M. Ruthven, Difussion of  $CO_2$  in 4A and 5A zeolites crystal, J. Colloid Interface Sci. 74 (1980) 186–195.
- [45] D. Saha, Z. Bao, F. Jia, S. Deng, Adsorption of CO<sub>2</sub>, CH<sub>4</sub>, N<sub>2</sub>O, and N<sub>2</sub> on MOF-5, MOF-177, and Zeolite 5A, Environ. Sci. Technol. 44 (2010) 1820–1826.
- [46] M.S.A. Baksh, R.T. Yang, Unique adsorption properties and potential energy profiles of microporous pillared clays, AIChE J. 38 (1992) 1357–1368.
- [47] C. Volzone, Retention of pollutant gases: comparison between clay, Appl. Clay Sci. 36 (2007) 191–196.
- [48] A. Möller, A. Pessoa Guimaraes, R. Gläser, R. Staudt, Uptake-curves for the determination of diffusion coefficients and sorption equilibria for n-alkaned on zeolites, Microporous Mesoporous Mater. 125 (2009) 23–29.
- [49] E. Fiani, L. Perier-Cambry, G. Thomas, Non-isothermal modelling of hydrocarbon adsorption on a granulated active carbon, J. Therm. Anal. Calorim. 60 (2000) 557–570.
- [50] D.M. Ruthven, Diffusion in type A zeolites: new insights from old data, Microporous Mesoporous Mater. 162 (2012) 69–79.
- [51] Y. Hua Ma, C. Mancel, Diffusion studies of CO<sub>2</sub>, NO, NO<sub>2</sub>, SO<sub>2</sub> on molecular sieve zeolites by gas chromatography, AlChE J. 18 (1972) 1148–1153.
- [52] Z. Bao, L. Yu, Q. Ren, X. Lu, S. Deng, Adsorption of CO<sub>2</sub> and CH<sub>4</sub> on a magnesium-based metal organic framework, J. Colloid Interface Sci. 353 (2011) 549–556.
- [53] M. Sahimi, Diffusion, adsorption, and reaction in pillared clays. I. Rod-like molecules in a regular pore space, J. Chem. Phys. 92 (1990) 5107–5118.
- [54] X. Yi, K.S. Shing, M. Sahimi, Molecular simulation of adsorption and diffusion in pillared clays, Chem. Eng. Sci. 51 (1996) 3409–3426.
- [55] A. Gil, S.A. Korili, F.C.C. Assis, M.A. Vicente, P. Eloy, E.M. Gaigneaux, New evidences on the relationship between the structure properties of pillared clays and their catalytic performance in the oxidation of benzene, in: J.R. González-Velasco, F. Ramoa-Ribeiro, A. Corma, J.L. Figueiredo (Eds.), Catalysis for a Sustainable World, Proceedings EuropaCat IX, Salamanca, Spain, 2009.
- [56] L. Hertag, H. Bux, J. Caro, C. Chmelik, T. Remsungnen, M. Knauth, S. Fritzsche, Diffusion of CH<sub>4</sub> and H<sub>2</sub> in ZIF-8, J. Membr. Sci. 377 (2011) 36–41.
- [57] Z.Y. Yeo, S.-P. Chai, P.W. Zhua, A.R. Mohamed, An overview: synthesis of thin films/membranes of metal organic frameworks and its gas separation performances, RSC Adv. 4 (2014) 54322–54334.
- [58] <a href="http://www.quantachrome.com/technical/dft.html">http://www.quantachrome.com/technical/dft.html</a>.
- [59] D. Saha, S. Deng, Adsorption equilibrium and kinetics of CO<sub>2</sub>, CH<sub>4</sub>, N<sub>2</sub>O, and NH<sub>3</sub> on ordered mesoporous carbon, J. Colloid Interface Sci. 345 (2010) 402– 409.
- [60] Z. Zhao, X. Li, Z. Li, Adsorption equilibrium and kinetics of P-xylene on chromium-based metal organic framework MIL-101, Chem. Eng. J. 173 (2011) 150–157.
- [61] K. Kamiuto, A. Goubaru, Ermalina, Diffusion coefficients of carbon dioxide within type 13X zeolites particles, Chem. Eng. Commun. 193 (2006) 628–638.